

## Does the emulsification procedure influence freezing and thawing of aqueous droplets?

Astrid Hauptmann, Karl F. Handle, Philipp Baloh, Hinrich Grothe, and Thomas Loerting

Citation: *J. Chem. Phys.* **145**, 211923 (2016); doi: 10.1063/1.4965434

View online: <http://dx.doi.org/10.1063/1.4965434>

View Table of Contents: <http://aip.scitation.org/toc/jcp/145/21>

Published by the [American Institute of Physics](#)

---

### Articles you may be interested in

[On the time required to freeze water](#)

*J. Chem. Phys.* **145**, 211922211922 (2016); 10.1063/1.4965427

[A physically constrained classical description of the homogeneous nucleation of ice in water](#)

*J. Chem. Phys.* **145**, 211915211915 (2016); 10.1063/1.4962355

[Effect of entropy on the nucleation of cavitation bubbles in water under tension](#)

*J. Chem. Phys.* **145**, 211918211918 (2016); 10.1063/1.4964327

[The surface charge distribution affects the ice nucleating efficiency of silver iodide](#)

*J. Chem. Phys.* **145**, 211924211924 (2016); 10.1063/1.4966018

---



**COMPLETELY  
REDESIGNED!**

**PHYSICS  
TODAY**

*Physics Today* Buyer's Guide  
Search with a purpose.

# Does the emulsification procedure influence freezing and thawing of aqueous droplets?

Astrid Hauptmann,<sup>1</sup> Karl F. Handle,<sup>1</sup> Philipp Baloh,<sup>2</sup> Hinrich Grothe,<sup>2</sup>  
and Thomas Loerting<sup>1,a)</sup>

<sup>1</sup>Institute of Physical Chemistry, University of Innsbruck, A-6020 Innsbruck, Austria

<sup>2</sup>Institute of Materials Chemistry, Vienna University of Technology, A-1060 Vienna, Austria

(Received 13 June 2016; accepted 5 October 2016; published online 28 October 2016)

Here we investigate the freezing and thawing properties of aqueous solutions in oil emulsions, with a particular focus on investigating the influence of the oil and surfactant and the stirring time of the emulsion. Specifically, we employ optical cryomicroscopy in combination with differential scanning calorimetry to study the phase behavior of emulsified 25 wt. % ammonium sulfate droplets in the temperature range down to 93 K. We conclude that the nucleation temperature does not vary with oil-surfactant combination, that is, homogeneous nucleation is probed. However, incomplete emulsification and non-unimodal size distribution of dispersed droplets very often result in heterogeneous nucleation. This in turn affects the distribution of freeze-concentrated solution and the concentration of the solid ice/ammonium sulfate mixture and, thus, the phase behavior at sub-freezing temperatures. For instance, the formation of letovicite at 183 K critically depends on whether the droplets have frozen heterogeneously or homogeneously. Hence, the emulsification technique can be a very strong technique, but it must be ensured that emulsification is complete, i.e., a unimodal size distribution of droplets near 15  $\mu\text{m}$  has been reached. Furthermore, phase separation within the matrix itself or uptake of water from the air may impede the experiments. © 2016 Author(s). All article content, except where otherwise noted, is licensed under a Creative Commons Attribution (CC BY) license (<http://creativecommons.org/licenses/by/4.0/>). [<http://dx.doi.org/10.1063/1.4965434>]

## INTRODUCTION

The technique of emulsifying aqueous solutions in oil matrices is widely used in various industries and scientific communities.<sup>1–16</sup> In industry, emulsions are used as liquid membrane systems,<sup>1</sup> as washing systems for textiles,<sup>2</sup> as a cutting fluid for metals,<sup>3</sup> to synthesize polymers and coatings by emulsion polymerization,<sup>4</sup> and also to remove overspray for coating booth.<sup>5</sup> Emulsions also play a role in the oil and gas industry, for example, to prevent the buildup of a hydrate plug by anti-agglomeration<sup>6</sup> or for quality control of the crude oil.<sup>7</sup> However, the formation of emulsions in the pipeline is rather unwanted as they will reduce the quality, increase the operating cost, cause corrosion to the transport system, and will contaminate the catalyst used for the refining process.<sup>8</sup> Furthermore, emulsions offer a huge potential in different food,<sup>9,10</sup> cosmetic and pharmaceutical applications<sup>11</sup> including creams,<sup>12</sup> encapsulation systems transporting important ingredients/active components,<sup>13</sup> or as taste-retaining fat-reducers.<sup>14</sup> In the scientific community of astrophysics, photographic emulsions are used to develop focal stellar images and to observe dark matter.<sup>15</sup> The freezing behavior of emulsions is particularly important in food, cosmetic, pharmaceutical, and automotive industries, which require products to be stored for a longer time and transported to various places at subzero temperatures. Emulsions in food must remain physically and chemically stable throughout

processing, freezing,<sup>16</sup> storage, and defrosting.<sup>17</sup> Depending on the food being processed, temperatures of 248 K in shock-freezing, between 223 K and 193 K in freeze-drying,<sup>9</sup> and 255 K/243 K for storage and transportation<sup>18</sup> are of special importance. Herein, the induction period of fat crystallization is a useful indicator for the freeze-thaw stability of food emulsions.<sup>19</sup> In the cosmetic industry, consumers are not recommended to store the products at subzero temperatures, though the industry itself is performing freeze-thaw stability tests on shampoos, pastes, and creams.<sup>20</sup> Concerning pharmaceutical emulsions, the storage and transport temperatures highly depend on the properties of the drug itself and on the manufacturing company's guidelines and legislations. Emulsions for external use (e.g., topical creams) undergo less stringent requirements than injected medication like intravenous lipid emulsion. Micro-emulsions at low temperatures also play an important role in the automotive industry, wherein they contribute to the shiny, water repellent coating on a tire<sup>21</sup> and also make the tire more durable in temperature fluctuations and shear forces.<sup>22</sup>

In the scientific community, emulsions are used in fundamental physico-chemical investigations on the anomalous properties of water, especially in order to avoid crystallization of the liquid or to suppress polymorphic transitions as long as possible. Moreover, particular interest is on emulsified droplets at subzero temperatures as a model system for aqueous droplets in the atmosphere, e.g., in the context of ice nucleation and cloud glaciation.<sup>23</sup> Analytical methods

<sup>a)</sup>E-mail: thomas.loerting@uibk.ac.at

to determine the freezing/thawing (FT) behavior of droplets by the emulsion techniques differ widely between research groups.

Table I shows a representative list of methods and techniques used by different scientific communities in order to analyze the FT behavior of water by emulsifying aqueous solutions. Complementary techniques, not based on emulsions, include levitating droplets (see Table II) or simply freezing water droplets on surfaces (see Table III).

The emulsion technique is a common technique among scientists who want to study the homogeneous freezing and thawing behavior of aqueous droplets, focusing on volume-dependent ice nucleation.<sup>24</sup> However, there have also been discourses about the influence of the surface in the nucleation process.<sup>23</sup> Results obtained from emulsion studies are taken with care, suspicion or even rejected by many researchers, especially because emulsions are complex systems and metastable in nature, demixing with

time. The segregation process is sketched schematically in Figure 1 and involves aggregation and coalescence of individual droplets, finally resulting in “sedimentation.” The driving force for this process is reduction of the interface (boundary layer). The process continues until both phases are completely separated (see Figure 1). Its rate can be estimated using Stokes’ law and depends quadratically on the radii of droplets. Thus, it is of high importance to produce droplets which are as small as possible for stable emulsions. A small density difference of the two phases as well as a high viscosity works in favor of stabilizing emulsions.<sup>25</sup>

Surfactants play a key role in stabilizing emulsions. A large range of surfactants are available, which can be distinguished based on their charges (non-ionic, cationic, anionic, amphoteric), solubilities, and the ratio of hydrophilic to lipophilic groups. Nonionic surfactants can be characterized by using the HLB (Hydrophile-Lipophile Balance) value. The

TABLE I. Representative examples of studies on W/O emulsions at subzero temperatures.

Matrix	Surfactant	Dispersed phase	Homogenization method	Lowest temperature (K)	Analytical method	Source
Canola oil	Polyglycerin polyricino-leate 3 wt. %	NaCl 30 wt. %	300 rpm propeller stirrer, colloid mill	213	DSC	26
Mineral oil	Lanolin 5 wt. %	Deionized water 20 wt. %	Homogeniser 7000 rpm 30 s	230	DSC	31
Methylcyclohexane	Span 80 2 wt. %	Triple-distilled water	Micro-fluidic device	223	DSC, cryomicroscopy	32
Paraffin oil	Lanolin 10 wt. %	45 wt. % Water plus pollen	Unspecified	233	Cryomicroscopy, SEM images	33
Halocarbon oil 0.8	Lanolin 20 wt. %	HNO <sub>3</sub> -H <sub>2</sub> SO <sub>4</sub> -H <sub>2</sub> O droplets	High-speed mixer	133	DSC	28
Mineral oil/nonadecanol solution	n.a.	Water droplets by droplet generator <sup>34</sup>		248	Optical microscopy, DSC	35
Paraffin oil	Lanolin 15-20 wt. %, Span 80, Atmos 300, Igepal CA420, Drewpol 10-4-O, Brij 92	Water droplets contain mineral dust particles, water of milli-Q-System.	Planetary mixer, water was added drop-wise	233/248	Cryomicroscopy, SEM, x-RD, IR spectroscopy, nitrogen adsorption, light microscopy with CCD camera	36
Halocarbon oil 0.8	Lanolin 20 wt. %	(NH <sub>4</sub> ) <sub>2</sub> SO <sub>4</sub> /H <sub>2</sub> O droplets	Unspecified	133	Cryomicroscopy	27
Mexican crude oil	n.a.	Distilled water 5%, 10%, 20% (v/v)	Crude oil heated to 213 K, shaking for 3 min	213	DSC	37
Silicone oil	(1) Span 80 0.05 wt. %, (2) Oil red O 0.05 wt. %	Deionized water	n.a.	Not spec. But sub-zero	Colour camera in microfluidic chip	38
Methylcyclohexane/methylcyclopentane	Span 65	Glycerol + water, water with Li salts, water 40% (v/v)	Stirring, gentle Heating <sup>39</sup>	~143/77	Raman spectroscopy, high pressure DTA, XRD, ESR, DTA	40
Heptane	Span 65 5 wt. %	Water (0.1 M CuCl <sub>2</sub> )	Heating/blender/motor-driven emulsifier	95		41
Heptan, cyclopentane THF, halocarbon oil 0.8	Span 65, lanolin	Distilled water	Vigorous shaking and ultrasoni-cation	233	DSC, optical microscopy	7
Methylcyclohexane/methylcyclopentane	Span 65	Methanol, ethylene glycol, glycerol, xylitol, poly(ethylene glycol)s, glucose, fructose	High-speed blender	~173	DSC, DTA	42

TABLE II. Representative examples of studies on levitated water droplets at subzero temperatures.

Sample analyzed	Applied procedure	Lowest temperature (K)	Analytical method	Research field and source
Water droplets (5 $\mu$ l)	On glass slides covered with superhydrophobic coatings under the condition of continuous spray	248	Transflective polarized microscopy	43
Water	Levitated in an electrodynamic balance	~233	Trap and CCD camera	44
Water droplets (6, 15, 30 $\mu$ l)	Gas diffusion layer in PEMFC performs the discharge of water vapor, contact with microporous surface and air	253	Monitoring with microscopy	45
Water droplets with desert dust samples	AIDA cloud simulation chamber, droplets and dust are levitated,	237	Welas optical particle counters, particle sizer, TDL absorption spectrometer	46
Water droplets and mineral dust particles	Continuous flow diffusion chamber (CFDC)	238	Optical particle counter	47
Aqueous ammonium sulfate droplets	Levitated by radiation pressure in air	213	Laser trapping–microspectroscopy system (+Raman)	48

higher the HLB value is, the more soluble is the surfactant in water.

There are two ways of stabilizing emulsions: Either by adding low-molecular weight surfactants or by adding macromolecular interface-active components (“protective colloids”). In this article, the focus is set on surfactants, which stabilize emulsions based on the development of adsorption layers that reduce the interface energy between the oil and the water phases. Surfactants consist of a hydrophilic and a hydrophobic part. In most cases, the surfactant is more soluble in one of both phases, which has an impact on the stability of the resulting emulsion. According to the Bancroft rule, the phase in which the surfactant is more soluble takes over the role of the dispersion medium, i.e., water/oil (W/O) emulsions are produced if the surfactant is more soluble in the oil phase. Solubilities are estimated on the basis of empirical

HLB values. A low HLB value means that the surfactant will tend to be oil-soluble and a surfactant with a high HLB value will tend to be water-soluble. In order to achieve a stable W/O emulsion, a HLB range of 4-6 is favorable. HLB values of the surfactants used in our study are listed in Table IV in the section titled “Materials and methods.”<sup>25</sup>

The stability of an emulsion also depends on the ratio of the inner (hydrophilic) and outer (hydrophobic) phases. If the volume of the inner phase falls below 30%, the effect that the droplets have on each other will be little and the physical properties will be determined by the dispersion medium. If the ratio exceeds 30%, single droplets interact with each other, the viscosity in the emulsion strongly increases and starts showing non-Newtonian flow behavior.<sup>25</sup> In the case of our experiments, we exclusively worked on emulsions with a low inner volume.

TABLE III. Representative examples of studies on water droplets deposited on surfaces at subzero temperatures.

Sample analyzed	Applied procedure	Lowest temperature (K)	Analytical method	Research field and source
Water droplets with rhodamine B	Impinging water droplets onto a red copper test plate (cooled down)	262	Fluorescence imaging by a CCD camera	49
Water, NaCl, HCl, NaOH droplets (2.7 mm and 3.5 mm diameter)	Cylindric vacuum-isolated cooling chamber, freezing between two wires, on one copper surface, between two copper plates	203	Oscilloscope measures voltage	50
Water droplets containing Snomax®	Separated droplets in individual compartments and frozen on glass surface, apparatus is called Bielefeld Ice Nucleation ARraY (BINARY)	263	Small arrays of cold-light white LEDs for contrast, images by a CCD camera	51
Water droplets (1 $\mu$ l) with mineral dust particles	$\mu$ l-nucleation by immersed particle instrument (NIPI), droplets on hydrophobic silanised glass slide	~233	NIPI with camera images	52
Ultra-pure water droplets (10-40 $\mu$ m diameter)	Droplets (nebulized water) were supported on a hydrophobic glass cover slip which had a hydrophobic organosilane coating	228	Optical microscopy	53

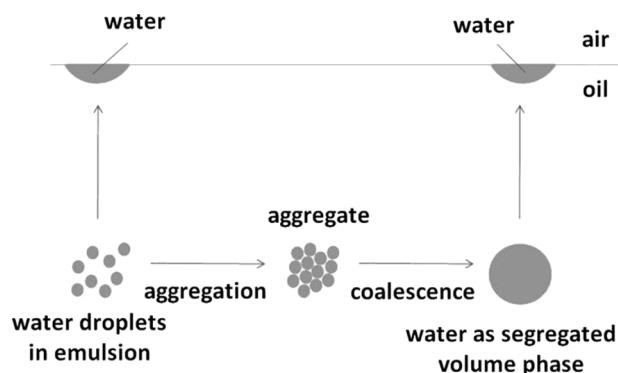


FIG. 1. Segregation process of emulsions.

Unstable emulsions can lead to a phase separation of the oil and water phases or to foaming wherein the biggest volume phase of the dispersion is gaseous. Figure 2 shows an optical microscope image of a foam that we encountered in our studies, namely, on the example of the Zonyl-FSN-100 surfactant in halocarbon 0.8 oil. Air bubbles of up to 300  $\mu\text{m}$  in diameter are seen in this example. The extent of foam formation is highly dependent on the frequency of the application of mechanical force (e.g., stirring rate), surfactants used, and other physical conditions like the temperature and time.

While parts of the scientific community consider the oil matrix and the surfactant as inert, not influencing the phase behavior of the emulsified droplets, others regard the influence to be highly significant.<sup>26</sup> Table I features a huge range of oils, spanning from canola oil via mineral oil and alkanes to halocarbon oils, and an even larger range of surfactants.

It is the purpose of this work to critically test the validity of the assumption that the interaction between aqueous and oil phases in emulsions is negligible by systematically varying the parameters of the emulsification procedure. To that end we here use optical cryomicroscopy observations in connection with differential scanning calorimetry (DSC) in the temperature range down to 93 K. We here have chosen an aqueous solution of 25 wt. % ammonium sulfate as our benchmark case. In this system, a very rich phase behavior was observed previously, featuring not only simple freezing and thawing of the droplets but also formation of freeze-concentrated solutions, cold-crystallization, and phase transformation to letovicite.<sup>27–30</sup> As oils we employed halocarbon oil 0.8, 1.8, 4.2, mineral oil, and methylcyclopentane/methylcyclohexane and as surfactants we employed Span 65, Span 83, lanolin, and Tween 80. These cover a large fraction of the ones used by the scientific communities in earlier studies (see Table I). In addition to the oils and surfactants themselves we also study the influence of the stirring time on the FT properties of the emulsion. The dispersion is reached by high-speed magnetic stirring in our experiments. Alternative dispersion methods, such as vortexing or ultrasonic bathing are used only for cases in which we were unable to produce an emulsion by magnetic stirring.

## MATERIALS AND METHODS

### Preparation of samples

As samples to be studied we first employed the pure oils, then oil/surfactant mixtures without aqueous phase, and

TABLE IV. Mixing ratios and preparation procedure of matrix and surfactant of W/O emulsions.

Matrix	Span 65 [%w/w] <i>HLB</i> = 2.1 <sup>54</sup>	Span 83 [%w/w] <i>HLB</i> = 3.7 <sup>55</sup>	Lanolin [%w/w] <i>HLB</i> = 4 <sup>56</sup>	Tween 80 [%w/w] <i>HLB</i> = 15 <sup>57</sup>	Homogenization procedure
Halocarbon oil 0.8	98/2 <sup>(1)</sup>	95/5 <sup>(2)</sup>	80/20 <sup>(3)</sup>		(1) Magnet stirrer, 17 min, 3000 rpm (2) Vortexing, 2 min, speed 10 (3) Ultrasonic bath, 10 min
Mineral oil		95/5 <sup>(4)</sup>	90/10 <sup>(5)</sup>	80/20 <sup>(6)</sup>	(4) Magnet stirrer, 17 h, 3000 rpm (5) Magnet stirrer, 5 min 3000 rpm (6) Magnet stirrer, 5 h, 2000 rpm (7) Magnet stirrer, 1 h, 3000 rpm
Methylcyclopentane/ methylcyclohexane (1:1)	93/7 <sup>(7)</sup>				

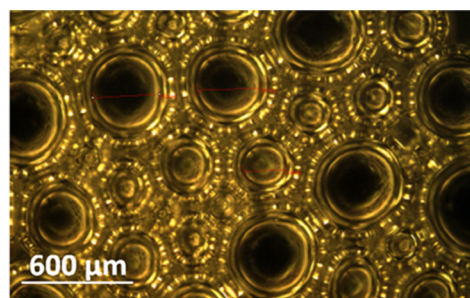
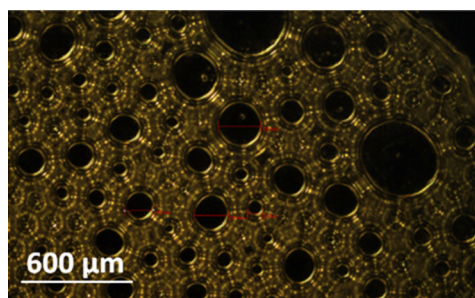


FIG. 2. Two exemplary optical cryomicroscopy images of a failed attempt to create a stable emulsion of Zonyl-FSN-100/halocarbon oil 0.8 (80:20) and ammonium sulfate (25 wt. %). The emulsion segregated after a very short time. The images display the top layer of the foamed matrix.

finally droplets of 25 wt. % ammonium sulfate (99.999%, CAS Number: 7783-20-2; Sigma-Aldrich, USA) in the matrix. The following oils were used as purchased by the vendor: halocarbon oil 0.8, halocarbon oil 1.8, and halocarbon oil 4.2 (99.9%, CAS Number 9002-83-9; Halocarbon Products Corporation, USA), white mineral oil (>99%, CAS Number 8042-47-5; Fisher Scientific, USA), methylcyclopentane (97%, CAS Number 96-37-7; Sigma-Aldrich, USA), and methylcyclohexane (99%, CAS Number 108-87-2; Merck & Co, USA).

Oil/surfactant samples (without dispersed phase) were prepared by mixing halocarbon oils (0.8, 1.8, and 4.2) with lanolin (CAS Number: 800-54-0; Sigma-Aldrich, USA) (90:10 wt. %). Homogenization was attempted by stirring the mixture with a 20 × 8 mm magnet stirrer for 35 min at ~2000 rpm. Additionally, methylcyclopentane and methylcyclohexane (1:1) was mixed with Span 65 (CAS Number: 26 658-19-5; Atlas Chemie, Germany) (7 wt. %) and homogenized by a 20 × 8 mm magnet stirrer for 30 min at ~2200 rpm.

W/O emulsions were prepared as listed in Table IV wherein the dispersed phase in all emulsions consists of 25 wt. % ammonium sulfate dissolved in double-deionized and distilled water. The aqueous phase was added to the oil/surfactant mixture in a 1:10 ratio. The surfactants Span 65, Span 83 (CAS Number: 8007-43-0; Sigma-Aldrich, USA), lanolin and Tween 80 (CAS Number: 900-65-6; Sigma-Aldrich, USA) were homogenized with the oil phase before the dispersed aqueous phase was added. In addition to stirring the emulsions with a magnet, we also employed a vortexer (Scientific Industries, Model K-550-GE) or ultrasonic bath for homogenization in exceptional cases (see Table IV).

All the W/O emulsion samples listed above were analyzed by DSC and additionally by optical cryomicroscopy. HLB values of the used surfactants are given in Table IV.

### DSC measurements

The application of calorimetric methods for characterization of emulsions was described by Rasmussen and MacKenzie<sup>39</sup> in the early 1970s. In our work two DSC devices were used: The DSC-4e (Perkin-Elmer, USA) and the DSC 8000 (Perkin-Elmer, USA). About 5-40  $\mu$ l of sample were loaded into an aluminum crucible, hermetically sealed and transferred to the instrument at ambient temperature. Alternatively, steel crucibles with a screw-on lid were used. The crucibles were then cooled to 160-90 K at a cooling rate of 3 K/min or 10 K/min, equilibrated for a few minutes at a low temperature and reheated again with the same rate to 285 K. Both instruments were first calibrated for correct transformation temperatures at subzero temperatures by using the recommended transitions in cyclopentane, cyclohexane, indium, and adamantane. Thereby the values of the recorded temperatures exhibit an accuracy of  $\pm 1$  K. The latent heat and the change in the heat capacity were calibrated using sapphire with an accuracy of  $\pm 0.1$  J/mol K.

### Optical cryomicroscopy measurements

An optical microscope BX-51 (Olympus Corporation, Japan) in combination with a temperature controlled Linkam cryostage LTS420 (Linkam Scientific Instruments, UK) was used to take images of the emulsion at temperatures as low as 93 K. A drop of emulsion was placed on the object plate and enclosed by a cover slip in order to prevent evaporation. Droplet size and size distribution were determined by calibrating an ULWD 50× objective (Olympus) and using the Linksys 32 software.

### RESULTS

The following result section shows mostly data that were retrieved from emulsions prepared by the magnetic stirring process. This method has proven to be most effective in most of our cases regarding the stability of emulsions. There are some exceptions where the emulsion was prepared by vortexing or ultrasonic bath.

Figure 3 reports cooling (left) and subsequent heating scans (right) for the pure oils. Ideally, no transitions at all should be observable for the oil to be suitable in studies at cryoconditions. In order to check for this we have used a high level of magnification (see scale bar in Figure 3) on the y-axis reporting the heat flow difference between the sample crucible and a reference crucible. At this level of magnification, even the baseline measured by comparing two “identical” crucibles is not straight and sometimes shows some effects, possibly caused by unavoidable impurities such as adsorption layers of water or other substances. Please note that the nature of the baseline is different from crucible to crucible, and the ones in Figure 3 (bottom) were chosen to be the worst examples of a “straight” baseline. The ideal case of no transitions at all is observed only in the case of halocarbon oil 0.8 (top traces). The wavy nature of the scan is a result of the high magnification and unavoidable differences between the reference crucible and the sample crucible. Baseline scans with two empty crucibles made either from aluminum or steel are exemplarily shown in the bottom panels of Fig. 3. It is evident that also the baselines have a wavy nature and may show sometimes spurious signals at this level of magnification. The other two halocarbon oils (traces 2 and 3 from top) are not suitable below about 170 K. Both oils show a glass transition as indicated by the sudden increase in heat flow corresponding to an increase in the heat capacity. The glass transition midpoint temperatures are marked by “ $T_g$ ” and are determined for halocarbon oil 1.8 to be 144 K and for halocarbon oil 4.2 to be 168 K. This corresponds to the temperature at which the oil becomes highly viscous, namely,  $10^{12}$  Pa s.<sup>58</sup> This difference of about 20 K in  $T_g$  is also reflected in the pour point of the halocarbon oils, which is 180 K for 1.8 and 200 K for 4.2. At the pour point, the viscosity becomes too high for the oil to be effectively poured out of its containment. The pour point for halocarbon oil 0.8 is 144 K, i.e., about 40 K lower than that for halocarbon oil 1.8. That is,  $T_g$  would be expected near 100 K. We do not see clear indications for a glass transition in halocarbon oil 0.8 down to 100 K. There is a very weak increase in the

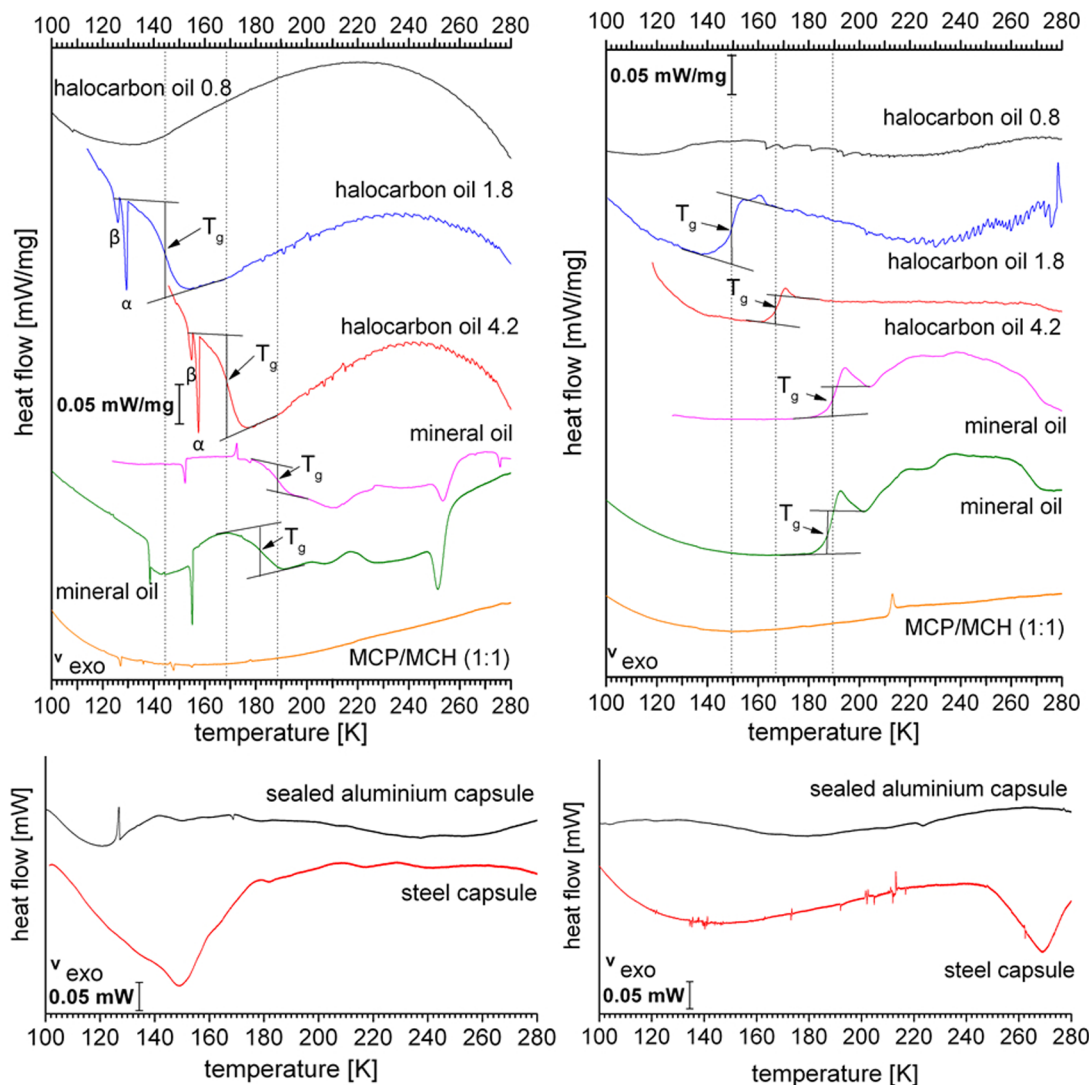


FIG. 3. (Top) Thermograms recorded by cooling (left)/heating (right) the pure oil at a rate of 10 K/min (methylcyclopentane and methylcyclohexane are abbreviated as MCP and MCH in the figures). The purple trace indicates the thermogram of mineral oil recorded with the DSC-4e and the green trace of mineral oil recorded with the DSC 8000 calorimeter. (Bottom) Examples for thermograms recorded by cooling (left)/heating (right) the empty DSC-capsules. Heat flow normalized to 1/10 of the capsule weight, for comparison with samples of mass 10 mg. Note, there are some effects at this strong magnification, which are caused by inequalities between two empty crucibles, e.g., impurities or deformations.

heat capacity in the heating scan near 120 K resembling a very subtle glass transition, though. Also the heating scan turns up a little bit in the cooling scan and could indicate a very subtle glass transition near 120 K. It is very hard to distinguish this from the baseline waves, though. We do not consider this to be a  $T_g$  because we would expect a change in the heat capacity similar to the one observed for the other two halocarbon oils, which is clearly not seen. All of the identified  $T_g$  and  $\Delta c_p$  of halocarbon oils 0.8, 1.8, and 4.2 and mineral oil are listed in Table V. For halocarbon oils 1.8 and 4.2, we see two additional exotherms that occur between the onset and the endpoint of the glass transition, first a more intense one and then a less intense one. Such exotherms usually indicate freezing — in this case the freezing of the oil or at least parts of the oil. Halocarbon oils are low molecular weight polymers of chlorotrifluoroethylene (PCTFE), and therefore these peaks could indicate the freezing or the agglomeration of some of the polymers. Crystallization within the glass transition range is not unusual. It was observed in many

materials, e.g., vitrified drug substances, alloys, or polymers.<sup>59</sup> As a consequence, the halocarbon oils can be used down to 180 K (4.2), 160 K (1.8), and 100 K (0.8) for emulsion studies.

Mineral oil, which is a mixture of higher alkanes and some aromatic components, shows a clear glass transition with a midpoint  $T_g$  at  $185 \text{ K} \pm 3 \text{ K}$  (cooling) and  $189 \text{ K} \pm 1 \text{ K}$  (heating). We have measured this oil not only in the DSC-4e instrument, but also in the DSC 8000 instrument to show the reproducibility and transferability of the method. The glass transition is clearly seen in the data from both instruments. Interestingly, the mineral oil shows an exothermic transition at about 250 K. We speculate that this transition could be associated with aggregation of some of the oil constituents. Methylcyclohexane/methylcyclopentane does not show any transitions at cooling, but shows a feature similar to a glass transition near 210 K transition upon heating (bottom trace). This is surprising since the calorimetric glass transition of methylcyclohexane is 85 K<sup>60</sup> and for methylcyclopentane

TABLE V. Glass transition midpoint temperatures  $T_g$  and heat capacity increases  $\Delta c_p$  extracted from Figure 3. The retrieved data were obtained by using the “tangent” evaluation which allows uncertainties of  $T_g \pm 3$  K and  $\Delta c_p \pm 0.1$ .

Pure substances	$T_g$ (K) (heating)	$T_g$ (K) (cooling)
Halocarbon oil 0.8	—	—
Halocarbon oil 1.8	150	144
Halocarbon oil 4.2	167	168
Mineral oil	189/188 <sup>a</sup>	188/182 <sup>a</sup>

Pure substances	$\Delta c_p$ [J/gK] (heating)	$\Delta c_p$ [J/gK] (cooling)
Halocarbon oil 0.8	—	—
Halocarbon oil 1.8	0.52	0.74
Halocarbon oil 4.2	0.23	0.78
Mineral oil	0.23/0.33 <sup>a</sup>	0.21/0.25 <sup>a</sup>

<sup>a</sup>Different DSC devices and different capsules (aluminum) used.

similar. However, we do not understand the origin of this feature.

Figure 4 shows the heating and cooling scan for oil/surfactant mixtures, in particular for the halocarbon oil/lanolin and methylcyclohexane-methylcyclopentane/Span 65 combinations. The ideal case is found for halocarbon oil 0.8/lanolin, in which no transitions are seen in the scans. Halocarbon oils 1.8 and 4.2 with lanolin are also good combinations, provided they are used above  $T_g$ . The glass transitions are also observed in Figure 4, marked by an arrow and  $T_g$ . Note that the increase in the heat capacity is markedly less compared to Figure 3 because these thermograms were recorded at 3 K/min as compared to 10 K/min. As a consequence, the same change in the heat capacity results in a heat flow change of only 3/10. Interestingly, the freezing of the oils is inhibited by the surfactant — the double-exotherm seen in Figure 3 is absent here. The surfactant impedes the crystallization of the oil phase possibly by restricting the mobility of oil molecules.

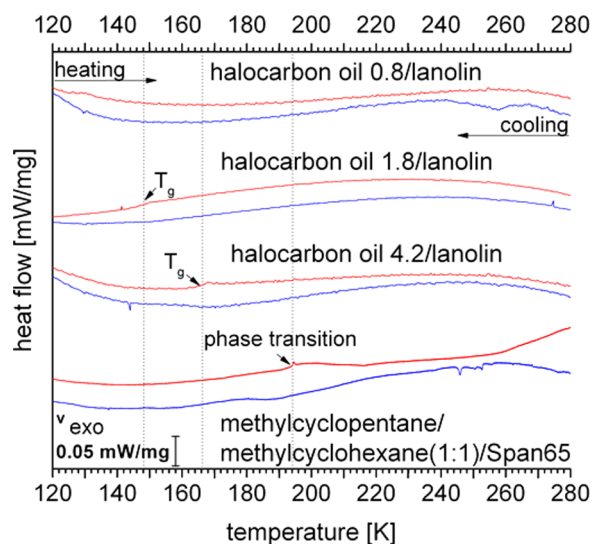


FIG. 4. Thermograms recorded by cooling/heating the oil-surfactant mixture at a rate of 3 K/min in a DSC instrument.

In the case of methylcyclohexane-methylcyclopentane/Span 65, the unexplained weak transition seen at 210 K in Figure 3 seems to shift to about 192 K because of the surfactant in Figure 4. The exothermic freezing events on the cooling curve (blue line) between 260 K and 240 K result from water taken up inadvertently by the emulsion. Indeed, water uptake by the emulsion is a key factor that is rarely mentioned in literature studies. This is exemplified on the example of halocarbon oil 0.8/lanolin below. Even though halocarbon oil 0.8/lanolin seems an ideal combination for studying aqueous droplets in emulsions at temperatures as low as 100 K, one has to be very careful. The DSC results presented in Figure 4 were obtained on samples in sealed crucibles. By contrast, the optical microscopy results shown in Figure 5 were obtained on samples inside the Linkam cryostage, which contains some ambient air. At ambient temperatures (panel (a)), the oil/surfactant is featureless on the  $\mu\text{m}$  length scale. The morphology of the matrix remains like this upon cooling at 10 K/min down to temperatures of 181 K, at which a first dark feature is visible (b). Upon continued cooling, the black spot converts rapidly to branched dark structures (c-e). Upon reheating from 123 K, the branched dark structures remain relatively unaffected up to about 253 K (e-k). At 263 K the previously sharp edges have become much smoother, so that a lot of the fine structure is lost (l). At the melting point of pure ice (m) and above (n-p) spherical droplets form. That is, the branched ice structures formed below 181 K melt into liquid droplets close to 273 K, and some “premelting” is seen below. This implies that the oil/surfactant combination has taken up some water from ambient air, and the water is most likely taken up by the hygroscopic lanolin. Even during the emulsification process (at ambient temperatures), before the FT-experiment itself is conducted, water may be taken up by the emulsions unless precautions are taken.

Also temperature gradients in the emulsion and transitions in the oil/surfactant matrix may play an important role in a freezing experiment, which are again rarely mentioned in the literature. One example of such a case is shown in Figure 6, which shows a sequence of cryomicroscopy images for an emulsion of 25 wt. % ammonium sulfate in halocarbon oil 0.8/Span 83. At 266.6 K (top left image), the emulsion has not yet changed from its appearance. Approximately 100 individual aqueous droplets clustered mainly in two regions of the image can be identified. The size distribution of the droplets is unimodal and ranges from approximately 8  $\mu\text{m}$  to 80  $\mu\text{m}$ . In between the droplet clusters, the oil/surfactant matrix is seen. This represents a good emulsion, well suitable for study of the freezing and thawing properties of the droplets. Upon cooling to below 255.2 K, we here observe some changes within the matrix itself, while the droplets remain unaffected. In particular, some structures slowly and progressively appear. At 255.1 K (top middle), very small structures of about 1  $\mu\text{m}$  appear within the matrix, but not everywhere in the matrix. Upon further cooling to 253.2 K (top right) and 246.4 K (middle left), these structures grow a little and spread over the whole matrix, while the droplets themselves still remain unaffected. The changes within the matrix cease upon further cooling: there is barely any difference between the images

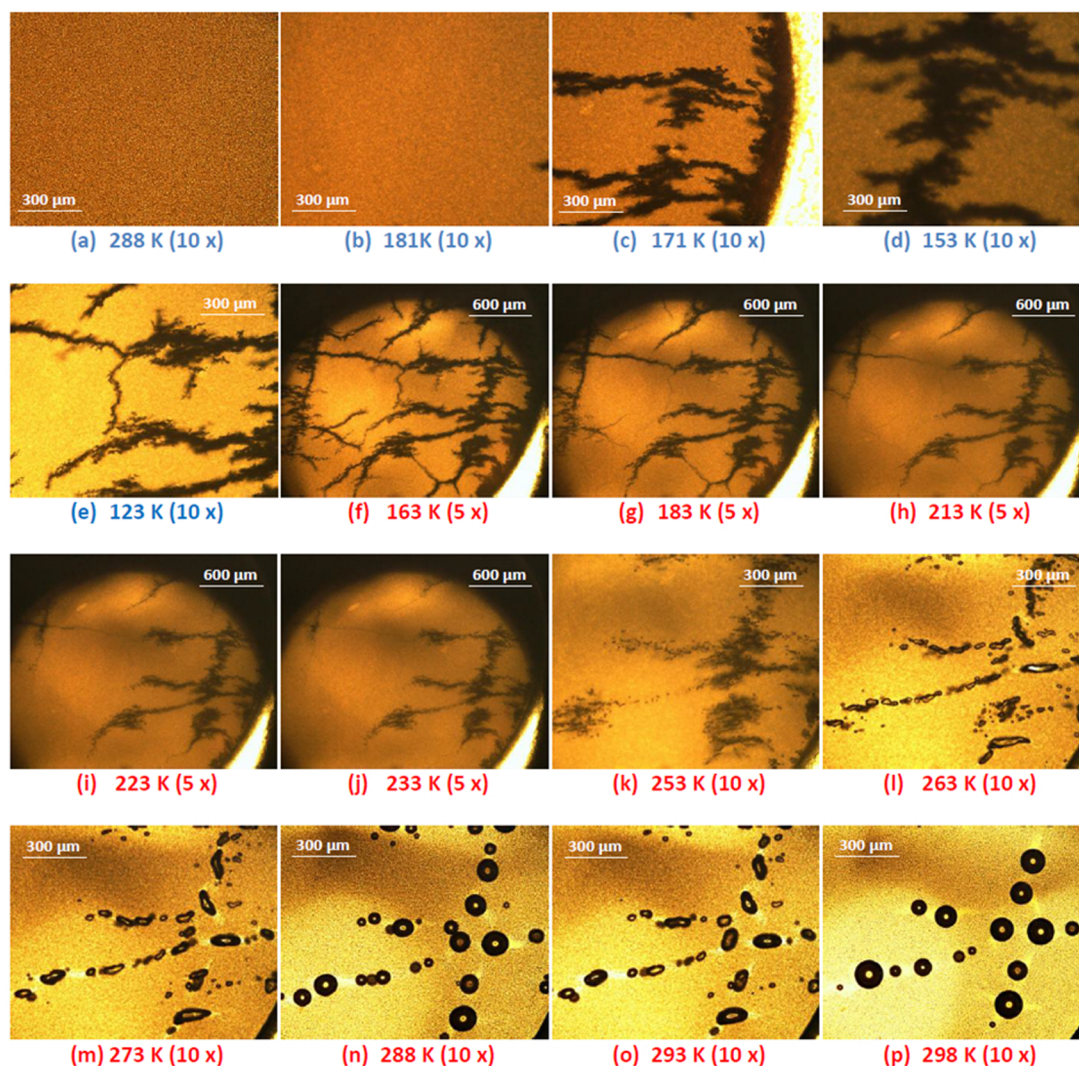


FIG. 5. Optical cryomicroscopy investigation of a pure halocarbon 0.8/lanolin 80:20 matrix cooled at 10 K/min. Temperatures upon cooling (blue) and heating (red) are indicated alongside the magnification of the objective.

recorded at 246.4 K and 226.7 K (center). The fact that the structures do not turn dark below the homogeneous freezing temperature of water of 235.2 K indicates that they are not condensing water droplets. We attribute the structuring within the matrix to precipitation of Span 83 within the halocarbon oil 0.8, presumably caused by the lower solubility of Span 83 in the oil at lower temperatures. We can rule out that there is a phase separation in the oil itself, first based on the DSC investigation shown in Figure 3. Second, such a kind of phase separation was not observed in any other oil/surfactant combination and also not in the pure oil itself in the cryomicroscopy experiments. This seems to be unique to the combination of halocarbon oil 0.8 with Span 83 at temperatures below about 255.2 K. Interestingly, we do not see such a phase separation in mineral oil in optical microscopy experiments but see an exotherm upon cooling at about 253 K (see Figure 3). This may imply that an aggregation or phase separation takes place within mineral oil, which is not visible on the  $\mu\text{m}$ -length scale accessible with the optical microscopy. Upon further cooling to 225.5 K (middle right), one of the large clusters of aqueous droplets suddenly freezes, as noticed by the sudden change of the

droplets from transparent to black. This result is within the range of the previously reported homogeneous nucleation temperature for 25 wt. % ammonium sulfate solutions between 227 and 211 K.<sup>61</sup> In our laboratories, we obtained freezing temperatures between 210 and 225 K for ammonium sulfate concentrations between 5% and 38%.<sup>62</sup> Comparing various results of different laboratories, ice nucleation temperatures of water droplets containing ammonium sulfate vary by over 15 K.<sup>63</sup> Nevertheless, the second large cluster of droplets does not freeze at the same temperature. This is likely the case because of a weak temperature gradient within the sample. We did not cool any lower than 225.5 K in the optical microscopy experiment shown in Fig. 6. Another less likely explanation is heterogeneous nucleation triggering the freezing event only in one cluster of droplets. Upon reheating, the melting of the frozen droplets proceeds in a quite different way: rather than a sudden change from black to transparent a stepwise change of contrast is seen, and several different shades of grey can be seen. The first noticeable change from black to gray is found near 243.2 K. At 248.8 K (bottom left), the frozen droplets now appear dark grey instead of black. This indicates partial melting of the droplets. At 259.3 K

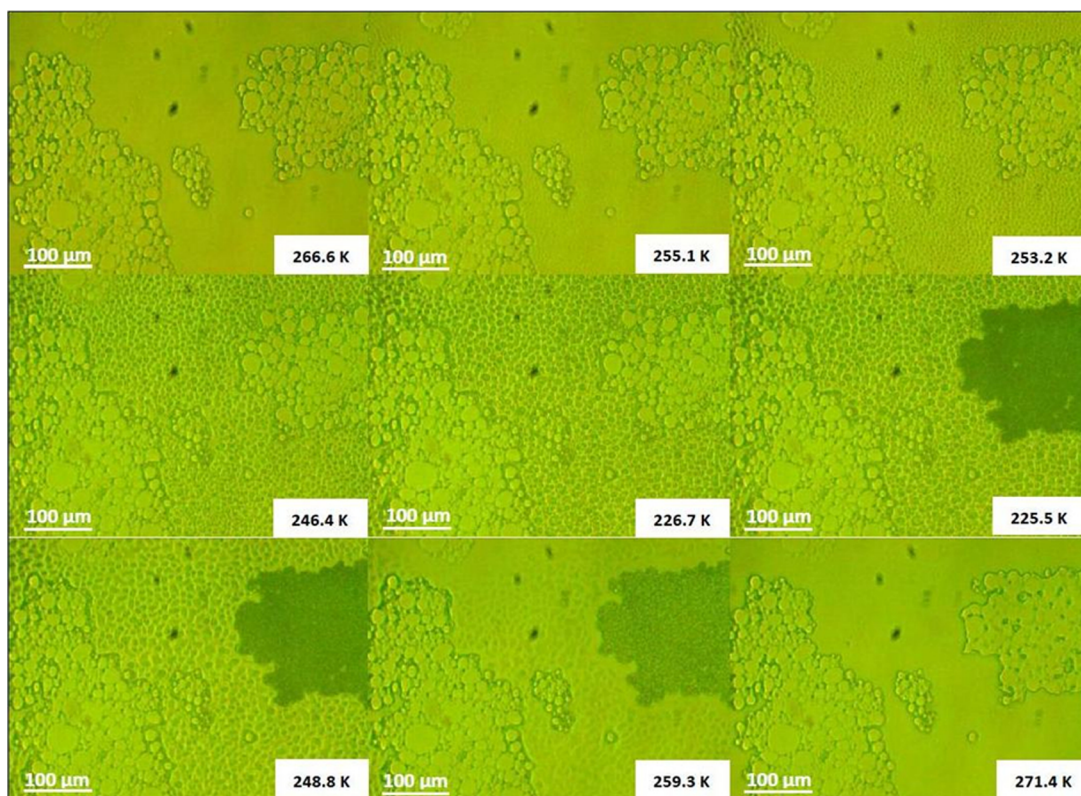


FIG. 6. Optical cryomicroscopy investigation of a halocarbon 0.8/Span 83 95:5 matrix with an aqueous dispersed phase containing 25% ammonium sulfate upon cooling to 225.5 K and reheating. Top two lines show selected images during cooling, bottom line during heating. Temperature is indicated in the individual images.

(bottom middle), the contrast has changed to light grey, i.e., the droplets have melted further, but still not completely. At 271.4 K, the droplets are transparent again, indicating that they are fully molten at this temperature again. This phenomenology is consistent with the findings of Bogdan *et al.*, who noticed a single freezing, but triple melting of frozen ammonium sulfate droplets, namely, melting of ice/letovicite, the eutectic solution of ammonium sulfate and ice/ammonium sulfate.<sup>27</sup> Please also note that the matrix itself has become smooth again at 271.4 K. That is, the phase separation of oil/surfactant was reversed. More precisely, the structuring within the matrix disappears at about 263.2 K. That is, there is some hysteresis between phase separation appearance (at 255.2 K) and disappearance (at 263.2 K), consistent with the first-order nature of a phase separation process.

The influence of the droplet size distribution on the FT-properties is demonstrated in Figure 7. We show the results for six different matrices, both in terms of optical microscopy at ambient temperatures and in terms of cryo-DSC measurements. Inspecting the scale bars and the size of the droplets, it becomes immediately clear that there is a huge range of sizes encountered. For instance, the halocarbon 0.8/Span 83 emulsion shows several clusters of droplets of sizes similar to the ones shown in Figure 6. However, there are also some much larger droplets of about 1 mm in diameter. This is a sign that the emulsification is incomplete, in some region  $\mu\text{m}$ -sized droplets can be found, in other regions mm-sized. By contrast, all droplets are smaller than 20  $\mu\text{m}$  in

diameter for mineral oil/lanolin or halocarbon oil 0.8/Span 65. We note that other combinations of oil/surfactant did not provide any emulsification at all — we, for instance, saw the formation of foams, i.e., bubbles of air inside the oil, instead of emulsions (see Figure 2). The result of the non-unimodal distribution of droplet sizes becomes clearly evident in the calorimetry scans in Figure 7. Most notably, there are emulsions in which we see up to 10 exothermic freezing events (halocarbon 0.8/Span 83) between 253 K and 223 K, whereas in others we see only a single freezing event close to 223 K (mineral oil/lanolin, halocarbon oil 0.8/Span 65). The reason for this is the size-dependence of the freezing event and the volume dependence of nucleation. In other words, the larger droplets freeze heterogeneously, whereas the micron-sized droplets freeze homogeneously near 223 K. This is particularly disturbing because it has been shown that the freezing behavior for micrometer-sized droplets is fundamentally different from millimeter-sized droplets:<sup>29</sup> while the former freeze homogeneously the latter experience two distinct freezing events, namely, the freezing out of ice at higher temperatures (240–250 K) and the freezing out of the residual freeze-concentrated solution at lower temperatures (210–215 K). The transition from ferroelectric ammonium sulfate crystals to paraelectric ammonium sulfate at 223 K can only be seen for the large millimeter-sized droplets, whereas it is absent in the smaller micrometer-sized droplets.<sup>30</sup>

Not only do we observe different freezing onset temperatures using the same content of aqueous phase, but we

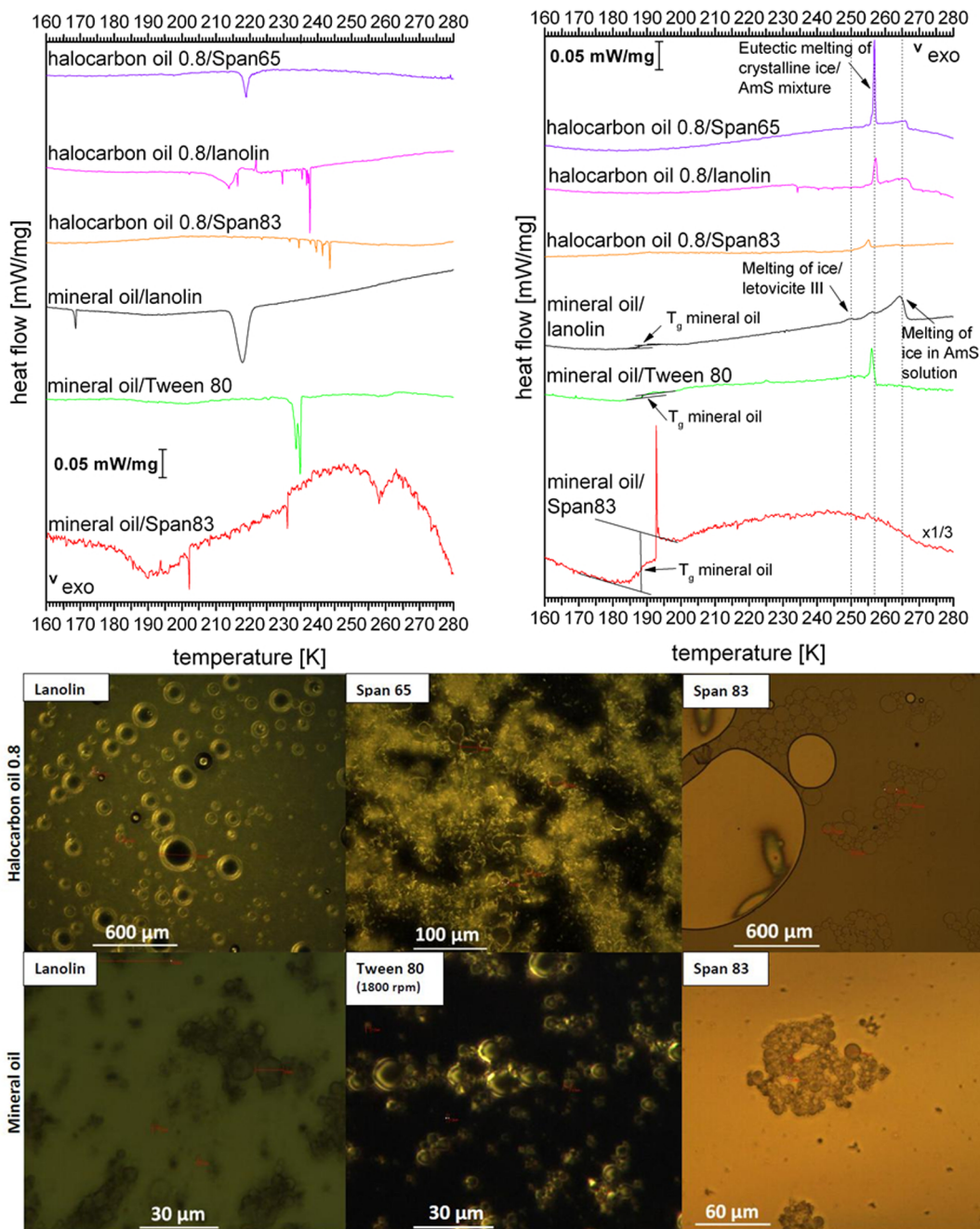


FIG. 7. Upper section shows thermograms recorded by cooling/heating W/O emulsions that contain dispersed water phase (1:10) with 25% ammonium sulfate measured at a rate of 3 K/min in a DSC instrument. Lower section shows cryomicroscopy images of the following W/O emulsions after stirring with  $10 \times 3$  mm magnet at 3000 rpm (with exception of halocarbon oil 0.8/lanolin which was dispersed in an ultrasonic bath).

also notice different thawing properties of different emulsions. While the melting temperatures are more or less the same, there is a major difference concerning the area/height of the endotherm and the sharpness. This size dependence of the freezing event has an impact on the formation of the freeze concentrated solutions and further on the transformation to letovicite at a much lower temperature (at 193 K). The three known melting events are indicated in Figure 7 (right) using dashed vertical lines. The appearance of the first peak which is the ice/letovicite eutectic melting peak at about 250 K is only found for good emulsions, e.g., mineral oil/lanolin. This peak and also the peak at around 185 K (see Figure 8) reveal the presence of crystallization on warming. The second

peak at around 257 K indicates the eutectic melting of a mixture of crystalline ice/crystalline AmS. The ratio of the peaks indicating the other two melting events of crystalline ice/AmS and of ice in AmS solution clearly differs from emulsion to emulsion. For example, in mineral oil/Tween 80 it appears there is almost exclusively melting of eutectic crystalline ice/ammonium sulfate at 257 K, whereas the other two melting peaks are absent. By contrast, the melting of eutectic crystalline ice/ammonium sulfate at 257 K is barely seen for mineral oil/lanolin, whereas the broad melting peak of ice in liquid AmS solution dominates. That is, the size of the droplets within the emulsion has a tremendous impact on the phase separation between ice and freeze concentrated solution,

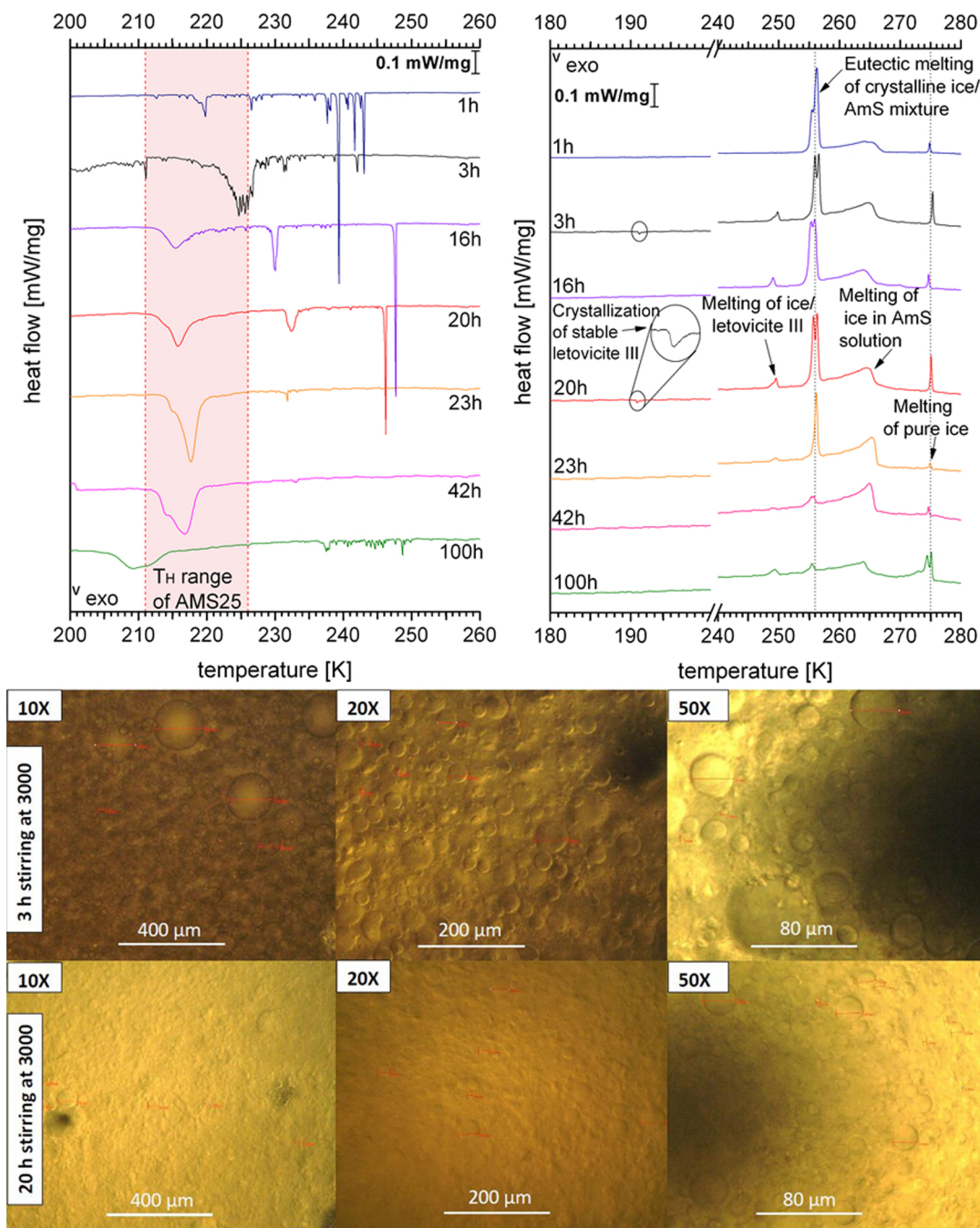


FIG. 8. Upper section shows thermograms recorded by cooling/heating W/O emulsions with methylcyclopentane/methylcyclohexane (1:1), Span 65 (7%), and a dispersed water phase (1:10) that consists of 25% ammonium sulfate stirred for variable time at 3000 rpm before measurement at a rate of 3 K/min in a DSC instrument (samples measured after 1 h and 16 h stirring are from a different batch). The light red region in thermograms of the cooling curves indicates the homogeneous freezing temperature (TH) range of the dispersed phase. Lower section shows cryomicroscopy images of W/O emulsions mentioned above after stirring with 10×3 mm magnet at 3000 rpm for 3 h and 20 h.

and upon continued cooling and reheating on the observed phase behavior. In more detail, the mutual distribution of ice and AmS differs from emulsion to emulsion. We envision that in mineral oil/lanolin, ice forms compact units that are enveloped by AmS, whereas the ice is distributed as much smaller units between AmS in mineral oil/Tween 80. As a consequence, all ice melts between 200 and 255 K for the latter emulsion, whereas the ice continuously melts in the former emulsion up to the equilibrium melting temperature of the 25 wt. % AmS solution of 265 K. The formation of

letovicite from ammonium sulfate was observed earlier and described in previous publications in detail.<sup>27,30,62</sup>

The impact of substrate (including mineral oil, Al<sub>2</sub>O<sub>3</sub>, lanolin wax, halocarbon oil 0.8, and various oil/surfactant-mixtures), of different surfaces and size of droplets on freezing events were previously analyzed by our group.<sup>29</sup> We concluded that the average freezing temperatures of ice and freeze-concentrated ammonium sulfate (25 wt. %) solution are quite similar in spite of the broad range of surfaces and substrates tested. Additionally, the mass of droplets does not

impact on the appearance of the freezing events of ice and residual solution.

Figure 8 shows that these differences are not only found for different combinations of oils and surfactants, but also for one specified combination as a function of the stirring time. In particular, we have investigated the influence of stirring time on the freezing and thawing properties of a methylcyclohexane-methylcyclopentane/Span 65 emulsion with 25 wt. % ammonium sulfate as the aqueous phase for stirring times between 1 h and 100 h. After one hour of stirring at 3000 rpm, the emulsion is incomplete: more than a dozen sharp freezing events take place between 243 K and 223 K. Only the ones at the low temperature may be assigned to the homogeneous single freezing (see Figure 8, light red region in between dashed lines). After three hours of stirring, the freezing temperatures shift significantly down, with most of the droplets freezing near 223 K. However, there are still a few freezing events between 243 K and 233 K, most likely freezing out of pure ice, but not of residual solution. These exotherms are much smaller indicating that only a small fraction of droplets freezes in this temperature range, whereas after 1 h the majority of droplets were freezing in this temperature range. Even on the broad peak near 223 K, several individual freezing events can be identified from the sharp peak tips on top of the broad freezing event. That is, it is still not the homogeneous freezing, but the sequential freezing of ice and residual solution. In accord with these observations, the microscopy images in Figure 8 after 3 h of stirring show some droplets of up to 200  $\mu\text{m}$  in diameter (top left), whereas most droplets are on the order 20  $\mu\text{m}$  in size (top middle). In addition, there are also smaller droplets, of about 5  $\mu\text{m}$  in size (top right). After about 20 h of stirring all of the larger droplets are dispersed, and droplets larger than 40  $\mu\text{m}$  can no longer be found (bottom left and middle). Typically, the droplets are 15–20  $\mu\text{m}$  in diameter (bottom right). As a consequence, almost all droplets freeze homogeneously near 223 K. However, some droplets may still freeze heterogeneously at higher temperatures, as indicated by the sharp freezing peak in the thermograms at 16 h and 20 h. These may also be absent, as seen for 23 h and 40 h stirring time — here practically all droplets freeze homogeneously near 223 K which is within the reported temperature range. In some of the heating thermograms, a tiny feature attributable to the formation of letovicite near 183 K can be seen (see circles and magnification in inset). The occurrence of freezing peaks between 253 K and 233 K (Figure 8, left) is correlated with a splitting of the melting peak of eutectic ammonium sulfate/crystalline ice at 256 K (Figure 8, right). By contrast this splitting is absent, if all droplets freeze homogeneously at 223 K, e.g., 23 h and 42 h stirring time. The melting of letovicite III near 249 K<sup>27</sup> is detected in all heating scans, except for the incomplete emulsion after 1 h.

The melting peaks of ice at 273 K in Fig. 8, right indicate that there are pure ice crystals inside the DSC crucible. The water may have been taken up either inside the DSC crucible at low temperature or during emulsification at ambient temperature. The first cooling scan in Figure 8, left, allows discriminating between the two cases. After stirring

for 23 or 42 h there are no freezing peaks down to 235 K, i.e., the homogeneous nucleation temperature of pure water. By contrast, after 100 h of stirring many tiny freezing peaks are evident at 235–250 K. These correspond to the freezing of pure water taken up inadvertently at ambient conditions. This water may then either be in contact with the emulsion matrix only or in contact with the aqueous AmS droplets. For stirring times up to 42 h, the former is the case as the behavior of the AmS droplets is not influenced significantly by the additional water. However, the splitting of the melting peak at 273 K (Fig. 8, right) and the downshift of the homogeneous nucleation temperature (Fig. 8, left) in the scan after 100 h stirring indicates that some water taken up from the environment actually comes into contact with the aqueous AmS droplets, but still without a proper mixing. As a result some water droplets contain a little bit of AmS (i.e., they melt slightly below 273 K) and some of the AmS droplets become enriched in AmS due to drying upon freezing of the water (i.e., the homogeneous nucleation temperature shifts downward compared to the other DSC traces in Fig. 8, left).

An important aspect to notice is that the homogeneous freezing temperature of 25 wt. % ammonium sulfate remains constant to an accuracy of  $\pm 1$  K, the accuracy of our temperature control and measurements both in microscopy and calorimetry experiments. That is, no matter what kind of oil/surfactant combination is used, the homogeneous nucleation temperature remains unaffected. However, the homogeneous nucleation is only investigated if proper emulsification has been reached, which means if a unimodal size distribution with droplet sizes centered around 15–20  $\mu\text{m}$  has been achieved. In other words, the matrix does not interfere with homogeneous bulk nucleation. Nucleation processes triggered at the interphase between the matrix and the aqueous phase can be ruled out on this basis. That is, the emulsion technique is very useful for studies of, e.g., cloud glaciations, even if there is no oil phase in the atmosphere.

## CONCLUSIONS

We have investigated systematically the influence of oil, surfactant and stirring time on the freezing and thawing properties of emulsified aqueous ammonium sulfate. Most notably we find that the freezing temperature of the individual properties mainly is a function of the size of the individual droplets, where larger droplets freeze at much higher temperature than smaller droplets. Once a threshold of droplets of a diameter of about 15–20  $\mu\text{m}$  has been reached, all droplets of 25 wt. % ammonium sulfate freeze at the same temperature of about 223 K, independent of the type of oil or surfactant employed. That is, the homogeneous nucleation temperature is not influenced by the choice of the matrix. Therefore, the emulsification technique is very powerful, especially if evaporation of droplets needs to be avoided and if the stochastic nature of the nucleation process is investigated, i.e., if large numbers of droplets are required for statistics purposes.

However, the choice of the matrix has a tremendous influence on the size distribution of droplets. As also seen in Figure 4, the surfactant can prevent the crystallization processes or influence the phase transition temperature of the oil phase. For some combinations of oil and surfactant, emulsions cannot be prepared at all, e.g., foams may be produced instead of emulsions. For other combinations, it is extremely hard to reach the wanted size distribution, such that droplets exceeding 200  $\mu\text{m}$  in diameter are present even after hours of stirring. One needs to be certain how long the stirring time needs to be before a good emulsification is reached. In the example shown in Figure 8, the stirring time needs to be >20 h to ensure proper emulsification. Good combinations of the oil surfactant that can be recommended based on our study are halocarbon oil 0.8/Span 65, mineral oil/lanolin, and methylcyclohexane-methylcyclopentane/Span 65. In the former two examples, good emulsions can be reached readily after only a couple of hours stirring. For the latter, stirring times of >20 h need to be obeyed.

For studies of these emulsions at very low temperatures (<223 K), it is necessary to work under dry atmospheres. Under humid atmospheres condensation of water in the form of ice into the emulsions is noticed below about 193–183 K. The water uptake does not only occur at cryo-conditions within the microscope cryostat or the DSC crucible, but also during the emulsification process itself (see Figure 8, left, 100 h curve). Also the oil/surfactant matrix itself may experience phase transitions — some show phase separation at 253 K as exemplified in Figure 6. Furthermore, the glass transition of the oil itself, i.e., the sudden increase of its viscosity limits the temperature range suitable for studies (see Figure 3). For studies near liquid nitrogen temperature, the best oils are halocarbon 0.8 and methylcyclohexane/methylcyclopentane. Other halocarbon oils or mineral oils are already in the glassy or even (partly) crystallized state at such low temperatures.

We emphasize there are many more emulsification techniques, such as the technique of high-speed blending described by Kanno *et al.*,<sup>42</sup> which produce stable emulsions within minutes. Our study emphasizes that the emulsification procedure itself, including the choices of oil, surfactant, and stirring-time, is crucial for the outcome of the FT-experiment. However, if good emulsions are produced, the results are the same, no matter what the choice of oil/surfactant is. In other words, the oil and the surfactant do not influence or trigger the freezing events or subsequent phase transitions, but only the quality of the emulsion.

## ACKNOWLEDGMENTS

We are grateful to Anatoli Bogdan and Georg Hölzl for discussions and to the Austrian Science Fund FWF (Grant Nos. P26040 and I1392) and the Austrian Research Promotion Agency FFG (Bridge project EarlySnow) for financial support.

<sup>1</sup>N. Othman, H. Mat, and M. Goto, *J. Membr. Sci.* **282**(1–2), 171 (2006).

<sup>2</sup>K. Knopf and E. Schollmeyer, *Fett Wiss. Technol./Fat Sci. Technol.* **93**(2), 67 (1991).

- <sup>3</sup>V. F. Silva, L. N. Batista, E. De Robertis, C. S. C. Castro, V. S. Cunha, and M. A. S. Costa, *J. Therm. Anal. Calorim.* **123**(2), 973 (2016).
- <sup>4</sup>M. W. Noh and D. C. Lee, *Polym. Bull.* **42**(5), 619 (1999); L. Yang, S. X. Zhou, and L. M. Wu, *Prog. Org. Coat.* **85**, 208 (2015).
- <sup>5</sup>W. J. Farrah and J. W. Pease, “Overspray removal systems for coating booths or the like,” U.S. patent 5,019,138 (28 May 1991).
- <sup>6</sup>Z. Huo, E. Freer, M. Lamar, B. Sannigrahi, D. M. Knauss, and E. D. Sloan, Jr., *Chem. Eng. Sci.* **56**(17), 4979 (2001).
- <sup>7</sup>Y. Zhang, P. G. Debenedetti, R. K. Prud’homme, and B. A. Pethica, *J. Phys. Chem. B* **108**(43), 16717 (2004).
- <sup>8</sup>S. F. Wong, J. S. Lim, and S. S. Dol, *J. Pet. Sci. Eng.* **135**, 498 (2015).
- <sup>9</sup>E. K. Silva, V. M. Azevedo, R. L. Cunha, M. D. Hubinger, and M. A. A. Meireles, *Food Hydrocolloids* **56**, 71 (2016).
- <sup>10</sup>A. A. Sharipova, S. B. Aidarova, D. Grigoriev, B. Mutaliev, G. Madibekova, A. Tleuova, and R. Miller, *Colloids Surf. B* **137**, 152 (2016); A. M. Talhat, V. Y. Lister, G. D. Moggridge, J. R. Rasburn, and D. I. Wilson, *J. Food Eng.* **156**, 67 (2015).
- <sup>11</sup>N. M. Hadzir, M. Basri, M. B. A. Rahman, A. B. Salleh, R. Z. R. A. Rahman, and H. Basri, *AAPS PharmSciTech* **14**(1), 456 (2013); G. L. Fell, P. Nandivada, K. M. Gura, and M. Puder, *Adv. Nutr.: Int. Rev. J.* **6**(5), 600 (2015).
- <sup>12</sup>M. S. Korenfeld, S. M. Silverstein, D. L. Cooke, R. Vogel, and R. S. Crockett, *J. Cataract Refractive Surg.* **35**(1), 26 (2009).
- <sup>13</sup>N. R. Maciel, E. C. Vargas Oliveira, C. H. Okuma, J. F. Topan, L. Q. Amaral, and P. Rocha-Filho, *J. Dispersion Sci. Technol.* **37**(5), 646 (2016); S. Sugiura, T. Kuroiwa, T. Kagota, M. Nakajima, S. Sato, S. Mukataka, P. Walde, and S. Ichikawa, *Langmuir* **24**(9), 4581 (2008); R. J. Prankerd and V. J. Stella, *PDA J. Pharm. Sci. Technol.* **44**(3), 139 (1990), available online at <http://journal.pda.org/content/44/3/139.abstract?sid=04d14a58-c038-4a67-bb59-4b984f794abf>.
- <sup>14</sup>B. C. Wu and D. J. McClements, *Food Res. Int.* **76**, 777 (2015); L. Román, M. M. Martínez, and M. Gómez, *ibid.* **74**, 72 (2015).
- <sup>15</sup>V. A. Ditlov, *Radiat. Meas.* **50**, 7 (2013); A. F. J. Moffat, *Astron. Astrophys.* **3**(4), 455 (1969).
- <sup>16</sup>L. Ramin, M. Mehranian, and F. Vahabzadeh, *Iran. J. Chem. Eng. (IJChE)* **6**(2), 3 (2009); A. E. Edris, *Food/Nahrung* **42**(01), 19 (1998), available online at [http://www.ijche.com/article\\_10357\\_1699.html](http://www.ijche.com/article_10357_1699.html).
- <sup>17</sup>B. M. Degner, C. Chung, V. Schlegel, R. Hutkins, and D. J. McClements, *Compr. Rev. Food Sci. Food Saf.* **13**(2), 98 (2014).
- <sup>18</sup>Q. Zhao, W. Kuang, M. Fang, D. Sun-Waterhouse, T. Liu, Z. Long, and M. Zhao, *Food Sci. Technol.* **62**(1), 287 (2015).
- <sup>19</sup>Y. Miyagawa, T. Ogawa, K. Nakagawa, and S. Adachi, *J. Oleo Sci.* **64**(11), 1169 (2015).
- <sup>20</sup>Cosmetics Europe, “Guidelines on stability testing of cosmetic products,” CTFA (2004), see <https://www.cosmetics-europe.eu/publications-cosmetics-europe-association/guidelines.html?view=item&id=20>.
- <sup>21</sup>T. C. Huang and R. L. Fausnight, “Silicone compositions for use in tire dressing and methods of making,” U.S. patent 7,074,262 (11 July 2006).
- <sup>22</sup>W. Obrecht, J.-P. Lambert, M. Happ, C. Oppenheimer-Stix, J. Dunn, and R. Krüger, *Ullmann’s Encyclopedia of Industrial Chemistry* (Wiley-VCH Verlag GmbH & Co. KGaA, 2000).
- <sup>23</sup>A. Tabazadeh, Y. S. Djikaev, and H. Reiss, *Proc. Natl. Acad. Sci. U. S. A.* **99**(25), 15873 (2002).
- <sup>24</sup>T. Bartels-Rausch, V. Bergeron, J. H. E. Cartwright, R. Escribano, J. L. Finney, H. Grothe, P. J. Gutiérrez, J. Haapala, W. F. Kuhs, J. B. C. Pettersson, S. D. Price, C. I. Sainz-Díaz, D. J. Stokes, G. Strazzulla, E. S. Thomson, H. Trinks, and N. Uras-Aytemiz, *Rev. Mod. Phys.* **84**(2), 885 (2012).
- <sup>25</sup>H. D. Dörfler, *Grenzflächen- und Kolloidchemie* (Wiley-VCH Verlag GmbH & Co. KGaA, 1994).
- <sup>26</sup>A. Schuch, K. Kohler, and H. P. Schuchmann, *J. Therm. Anal. Calorim.* **111**(3), 1881 (2013).
- <sup>27</sup>A. Bogdan, M. J. Molina, H. Tenhu, and T. Loerting, *Phys. Chem. Chem. Phys.* **13**(44), 19704 (2011).
- <sup>28</sup>A. Bogdan, M. J. Molina, H. Tenhu, E. Mayer, and T. Loerting, *Nat. Chem.* **2**(3), 197 (2010).
- <sup>29</sup>A. Bogdan and T. Loerting, *J. Phys. Chem. C* **115**(21), 10682 (2011).
- <sup>30</sup>A. Bogdan, M. J. Molina, H. Tenhu, T. Petäjä, and T. Loerting, *J. Phys. Chem. C* **116**(16), 9372 (2012).
- <sup>31</sup>V. Pinti, C. Marcolli, B. Zobrist, C. R. Hoyle, and T. Peter, *Atmos. Chem. Phys.* **12**(13), 5859 (2012).
- <sup>32</sup>B. Riechers, F. Wittbracht, A. Hutten, and T. Koop, *Phys. Chem. Chem. Phys.* **15**(16), 5873 (2013).
- <sup>33</sup>B. G. Pummer, H. Bauer, J. Bernardi, S. Bleicher, and H. Grothe, *Atmos. Chem. Phys.* **12**(5), 2541 (2012).

- <sup>34</sup>D. A. Knopf and T. Koop, *J. Geophys. Res.: Atmos.* **111**(D12), D12201, doi:10.1029/2005JD006894 (2006).
- <sup>35</sup>B. Zobrist, T. Koop, B. P. Luo, C. Marcolli, and T. Peter, *J. Phys. Chem. C* **111**(5), 2149 (2007).
- <sup>36</sup>T. Zolles, J. Burkart, T. Häusler, B. Pummer, R. Hitznerberger, and H. Grothe, *J. Phys. Chem. A* **119**(11), 2692 (2015); M. P. Aronson, K. Ananthapadmanabhan, M. F. Petko, and D. J. Palatini, *Colloids Surf. A* **85**(2-3), 199 (1994).
- <sup>37</sup>J. A. Díaz-Ponce, E. A. Flores, A. Lopez-Ortega, J. G. Hernández-Cortez, A. Estrada, L. V. Castro, and F. Vazquez, *J. Therm. Anal. Calorim.* **102**(3), 899 (2010).
- <sup>38</sup>A. E. Sgro and D. T. Chiu, *Lab Chip* **10**(14), 1873 (2010).
- <sup>39</sup>D. H. Rasmussen and A. P. MacKenzie, *J. Chem. Phys.* **59**(9), 5003 (1973).
- <sup>40</sup>Y. Suzuki and O. Mishima, *J. Chem. Phys.* **141**(9), 094505 (2014); C. A. Angell, E. J. Sare, J. Donnella, and D. R. MacFarlane, *J. Phys. Chem.* **85**(11), 1461 (1981); O. Mishima and H. E. Stanley, *Nature* **392**(6672), 164 (1998).
- <sup>41</sup>P. Brüggele and E. Mayer, *Nature* **288**(5791), 569 (1980).
- <sup>42</sup>H. Kanno, K. Miyata, K. Tomizawa, and H. Tanaka, *J. Phys. Chem. A* **108**(28), 6079 (2004).
- <sup>43</sup>J. Hu, K. Xu, Y. Wu, B. Lan, X. Jiang, and L. Shu, *Appl. Surf. Sci.* **317**, 534 (2014).
- <sup>44</sup>P. Stöckel, I. M. Weidinger, H. Baumgärtel, and T. Leisner, *J. Phys. Chem. A* **109**(11), 2540 (2005).
- <sup>45</sup>C.-W. Park, D.-G. Lee, J.-H. Peck, and C.-D. Kang, *Korean J. Air-Cond. Refrig. Eng.* **23**(3), 173 (2011).
- <sup>46</sup>M. Niemand, O. Möhler, B. Vogel, H. Vogel, C. Hoose, P. Connolly, H. Klein, H. Bingemer, P. DeMott, J. Skrotzki, and T. Leisner, *J. Atmos. Sci.* **69**(10), 3077 (2012).
- <sup>47</sup>A. Salam, U. Lohmann, B. Crenna, G. Lesins, P. Klages, D. Rogers, R. Irani, A. MacGillivray, and M. Coffin, *Aerosol Sci. Technol.* **40**(2), 134 (2007).
- <sup>48</sup>S. Ishizaka, T. Wada, and N. Kitamura, *Chem. Phys. Lett.* **506**(1-3), 117 (2011).
- <sup>49</sup>Z. Jin, S. Jin, and Z. Yang, *J. Visualization* **16**(1), 13 (2013).
- <sup>50</sup>S. Bauerecker and T. Buttersack, *J. Phys. Chem. B* **118**(47), 13629 (2014).
- <sup>51</sup>C. Budke and T. Koop, *Atmos. Meas. Tech.* **8**(2), 689 (2015).
- <sup>52</sup>T. F. Whale, B. J. Murray, D. O'Sullivan, T. W. Wilson, N. S. Umo, K. J. Baustian, J. D. Atkinson, D. A. Workneh, and G. J. Morris, *Atmos. Meas. Tech.* **8**(6), 2437 (2015).
- <sup>53</sup>B. J. Murray, S. L. Broadley, T. W. Wilson, S. J. Bull, R. H. Wills, H. K. Christenson, and E. J. Murray, *Phys. Chem. Chem. Phys.* **12**(35), 10380 (2010).
- <sup>54</sup>C. Balestra, S. Biancolini, R. Biavasco, D. Ferraro, A. Gunnella, and L. Tavella, "Ink-jet recording material," U.S. patent 7,862,868 (27 July 2006).
- <sup>55</sup>B. Evans, C. Morris, and D. B. Hagan, "Cosmetic composition containing alpha hydroxy carboxylic acids as preservatives," European patent 0568307 (3 November 1993).
- <sup>56</sup>Deutsche Lanolin Gesellschaft, retrieved from <http://www.parmentier.de/lanolin/hlb> (accessed 22 May 2016).
- <sup>57</sup>D. F. H. Chowdhury, "Surfactant vesicles," international patent WO2012049488 (19 April 2012).
- <sup>58</sup>P. G. Debenedetti, *Metastable Liquids—Concepts and Principles* (Princeton University Press, 1996).
- <sup>59</sup>J. W. P. Schmelzer, *Glass: Selected Properties and Crystallization* (De Gruyter, 2014).
- <sup>60</sup>C. A. Angell, J. M. Sare, and E. J. Sare, *J. Phys. Chem.* **82**(24), 2622 (1978).
- <sup>61</sup>B. H. Larson and B. D. Swanson, *J. Phys. Chem. A* **110**(5), 1907 (2006).
- <sup>62</sup>A. Bogdan, M. J. Molina, H. Tenhu, E. Mayer, E. Bertel, and T. Loerting, *J. Phys.: Condens. Matter* **23**(3), 035103 (2011).
- <sup>63</sup>A. K. Bertram, T. Koop, L. T. Molina, and M. J. Molina, *J. Phys. Chem. A* **104**, 584 (2000); J. H. Chelf and S. T. Martin, *J. Geophys. Res.: Atmos.* **106**(D1), 1215, doi: 10.1029/2000JD900477 (2001); D. J. Cziczko and J. P. D. Abbatt, *ibid.* **104**(D11), 13781, doi: 10.1029/1999JD900112 (1999); A. J. Prenni, M. E. Wise, S. D. Brooks, and M. A. Tolbert, *ibid.* **106**(D3), 3037, doi: 10.1029/2000JD900454 (2001); Y. L. Chen, P. J. DeMott, S. M. Kreidenweis, D. C. Rogers, and D. E. Sherman, *J. Atmos. Sci.* **57**(22), 3752 (2000); H. M. Hung, A. Malinowski, and S. T. Martin, *J. Phys. Chem. A* **106**(2), 293 (2002); H. M. Hung and S. T. Martin, *J. Geophys. Res.: Atmos.* **106**(D17), 20379, doi:10.1029/2000JD000212 (2001).